Closed-form suboptimal maximum-likelihood sequence detection for free-space optical communications

Lu Zhang[1,2,*] and Zhiyong Wu[1]

[1]Changchun Institute of Optics, Fine Mechanics and Physics, Chinese Academy of Sciences, Changchun, Jilin 130033, China

[2]Graduate University of Chinese Academy of Sciences, Beijing 10049, China

*Corresponding author: LZhangpai@gmail.com

Received 27 June 2012; revised 9 August 2012; accepted 9 August 2012; posted 14 August 2012 (Doc. ID 171496); published 11 September 2012

In this paper, a closed-form suboptimal maximum-likelihood sequence detection (MLSD) metric and its low-complexity version are proposed for free space optical communications systems operating over log-normal fading and high signal-to-noise channel. This algorithm provides a simplification to the algorithm reported by Riediger *et al.* In comparison, firstly, the parameters of this algorithm are independent of the scintillation index's variation, and secondly this algorithm just contains conventional computations; it saves computational time significantly. Bit error rate performance results confirm that the proposed algorithm performs comparably well as optimal MLSD. Moreover, the low-complexity version of this algorithm consumes much less time than the previously suboptimal MLSD metric presented by Riediger *et al.* © 2012 Optical Society of America

OCIS codes: 060.2605, 040.1880, 010.1330.

1. Introduction

Free space optical (FSO) systems operating over a turbulent atmosphere channel experience fading of the received optical signal, which severely affects the reliability of the FSO link. Currently, the on-off keying (OOK) intensity modulation (IM) and direct detection (DD) are mainly employed for commercial FSO systems. For such systems, a great deal of previous research has assumed that the receiver had perfect knowledge of the instantaneous fading intensity [1–4]. However, in practical implementation, the fading intensity is usually estimated using either the received sequence only [5–9] or redundant overhead, such as training sequences or pilot symbols [10–13]. FSO links possess correlation times of several to hundreds of milliseconds, resulting in a channel that is stationary for millions of bits at a Gbps rate. Hence, a simple channel estimation (using as few as 50 bits) can be used to estimate the channel state. Once the information of such a channel state isavailable, a simple threshold test can be used to render a decision regarding the transmitted bits for a duration of several million bits. Even in the bandwidth-hungry, sub-Gbps RF wireless channels, pilot symbols are used to reduce the complexity. Detection techniques with no channel state information have attracted the attention of academic research [14–16]. Zhu and Kahn [10,17,18] first investigated maximum-likelihood sequence detection (MLSD) in the context of FSO communications to recover the performance loss induced by symbol-by-symbol maximum-likelihood (ML) detection. Despite the fact that MLSD simply requires knowledge of the channel's fading statistics, it also requires that every sequence is detected using an unnecessarily complicated detection process and

1559-128X/12/276441-07$15.00/0
© 2012 Optical Society of America

therefore suffers from being highly complex [14–16]. MLSD is appropriate for a channel that cannot afford a few pilot symbols and the processing speed requirements are such that one will be able to explore a complicated MLSD approach. Consequently, to reduce the complexity, suboptimal MLSD metrics have been proposed in [14,15] for different detection models. In [14,15], because distribution approximation was introduced to derive the suboptimal MLSD metric, different distribution approximation parameters were necessary to compute as the scintillation index varies, therefore, it increased the complexity of the suboptimal MLSD metric. Moreover, it was difficult to calculate its parameters. Besides, the analytic decision metrics in [14,15] contain some complicated computations, such as computing the complementary error function and factorial, that are time consuming. Similarly, to address the complexity issue and to get rid of the dependent on the channel's fading statistics, another generalized maximum-likelihood sequence detection (GMLSD) suboptimal detection rule has been suggested by [16]. But in practical implementation, GMLSD requires at least one symbol in the transmitted sequence to correspond to the on state. Furthermore, GMLSD was only particularly effective for large sequence lengths; nevertheless, large sequence lengths result in immense computational time.

In this paper, to further simplify the algorithm presented by Riediger *et al.* [14], we develop a closed-form suboptimal MLSD metric and a reduced-complexity fast closed-form suboptimal MLSD metric for a high signal-to-noise (SNR) regime. After simplification, firstly, the parameters of the new algorithm are independent of scintillation index's variation, and secondly this algorithm does not contain complicated computations, such as computing complementary error function and factorial, which are time consuming. It just contains conventional computations. At the end of this paper, the performance of the proposed algorithm is investigated to demonstrate its merits.

2. Channel Fading Model

In a weak turbulence channel, the logarithm of the intensity variations is normally distributed and the probability density function (pdf) of I [14–16] is given by

$$p_I(I) = \frac{1}{I\sqrt{2\pi\sigma^2}} \exp\left\{-\frac{(\ln I + \sigma^2/2)^2}{2\sigma^2}\right\}, \quad (1)$$

with $\sigma^2 = \ln(\mathrm{S.I.} + 1)$ and S.I. being the scintillation index. Based on Eq. (1), $\mathrm{E}\{I\} = 1$ is satisfied.

For the signaling rates of interest, i.e., hundreds to thousands of Mbps, the fading intensity I can be treated as constant over the observation window, which means that all of the information-bearing bits in the same observation window experience the same I.

3. Received Signal Model

An FSO communications system employing IM/DD and OOK modulation is considered. It is assumed that the receiver operates in the high SNR regime. Hence, a Gaussian noise model is a good approximation of the Poisson photon counting detection model [14,17,19]. The photodetector of the FSO receiver converts the received optical field to electrical signal, which is integrated over each bit interval to produce a set of statistics suitable for detection. For the kth bit interval, the received discrete-time signal is given by [2,14,17]

$$r[k] = s[k]I + w[k], \quad (2)$$

with $s[k] \in \{0, 1\}$ being the transmitted OOK symbol, I being the channel fading coefficient due to atmospheric turbulence, and $w[k]$ being the additive white Gaussian noise. The mean and variance of $w[k]$ are 0 and σ_w^2 respectively.

Assuming static fading, the MLSD metric will detect a received sequence including N symbols from a window of N statistics. A window corresponding to bit interval indices $k = 1, 2, \ldots, N$ is considered. Let $\mathbf{r} \triangleq \{r[k]\}_{k=1}^N$ and $\mathbf{s} \triangleq \{s[k]\}_{k=1}^N$. Given the transmitted sequence $\mathbf{s}$ and channel fading coefficient I, the pdf of received vector $\mathbf{r}$ [14] is

$$p(\mathbf{r}|\mathbf{s}, I) = \prod_{k=1}^{N} p(r[k]|s[k], I), \quad (3)$$

where

$$p(r[k]|s[k], I) = \frac{1}{\sqrt{2\pi\sigma_w^2}} \exp\left\{-\frac{(r[k] - s[k]I)^2}{2\sigma_w^2}\right\}. \quad (4)$$

The average electrical SNR is defined as [2,14,17]

$$\gamma \triangleq \frac{E\{s[k]I\}^2}{E\{(w[k])^2\}} = \frac{\mu_I^2}{4\sigma_w^2}, \quad (5)$$

where $\mu_I = E\{I\}$ is the mean of the intensity, and all SNR employed in this paper are electrical.

4. Closed-Form Suboptimal MLSD Metric

An optimal MLSD metric [14] is given by

$$M_{\mathrm{opt}}(N_{\mathrm{on}}, R_{\mathrm{on}}) = \int_0^\infty \exp\left\{\frac{2R_{\mathrm{on}}I - N_{\mathrm{on}}I^2}{2\sigma_w^2}\right\} p_I(I)\mathrm{d}I, \quad (6)$$

where $N_{\mathrm{on}} \in \{0, 1, \ldots, N\}$ is the number of ones in the hypothesis vector, $R_{\mathrm{on}} \triangleq \sum_{n_i \in S_{\mathrm{on}}} r[n_i]$ is the sum of the received statistics that correspond to the indices of the ones in the hypothesis, and $S_{\mathrm{on}} \triangleq \{n_i \in \{1, 2, \ldots, N\} : s[n_i] = 1\}$ is the size-N_{on} set of on indices [14], and $p_I(I)$ is given by Eq. (1).

Change the variable of the integral in Eq. (6) to $\ln I$, and let $\varphi(N_{\mathrm{on}}, R_{\mathrm{on}}, I) = \exp[(2R_{\mathrm{on}}I - N_{\mathrm{on}}I^2)/2\sigma_w^2]$

and $q_m(N_{on},R_{on},I) = \partial^m \ln\varphi(N_{on},R_{on},I)/\partial(\ln I)^m$. Denote the integrand in Eq. (6) by $f(\ln I)$, thus, at the maximum point (i.e., stationary point) ξ, the stationary condition $\partial \ln f(\ln I)/\partial(\ln I)|_{I=\xi} = 0$ must be satisfied. So the stationary condition leads to

$$\ln \xi = -\frac{\sigma^2}{2} + \sigma^2 \frac{R_{on}\xi - N_{on}\xi^2}{\sigma_w^2}. \tag{7}$$

Using Eq. (7), the stationary point ξ can be obtained by iteration method.

At the point $\ln \xi$, expanding $\ln \varphi(N_{on},R_{on},I)$ in a Taylor series and letting $x = \ln(I/\xi)/\sigma$ yield

$$\begin{aligned}\varphi(N_{on},R_{on},I) &= \exp\{\ln \varphi(N_{on},R_{on},I)\}\\ &= \varphi(N_{on},R_{on},\xi)\exp(x\sigma q_1\\ &\quad + x^2\sigma^2 q_2/2)\exp(\varepsilon(x)),\end{aligned} \tag{8}$$

where the error term $\varepsilon(x)$ is of order $x^3\sigma^3 q_3$. The error term is little enough to neglect, then there is

$$\varphi(N_{on},R_{on},I) = \varphi(N_{on},R_{on},\xi)\exp(x\sigma q_1 + x^2\sigma^2 q_2/2). \tag{9}$$

Substituting $x = \ln(I/\xi)/\sigma$ into $p_I(I)dI$ in Eq. (6) and executing the integral yield the closed-form expression of suboptimal MLSD metric:

$$\begin{aligned}M_{\text{subopt}}(N_{on},R_{on}) &= \frac{\varphi(N_{on},R_{on},\xi)\exp(-\sigma^2 q_1^2/2)}{\sqrt{1-\sigma^2 q_2}}\\ &= \frac{\exp\{(2R_{on}\xi - N_{on}\xi^2)/2\sigma_w^2\}\exp(-\sigma^2 q_1^2/2)}{\sqrt{1-\sigma^2 q_2}}.\end{aligned} \tag{10}$$

For clarity, the algorithm for the closed-form suboptimal MSLD metric is summarized as follows:

(1) For $N_{on} = 0$, there is $M_{\text{subopt}}(N_{on},R_{on}) = 1$.
(2) For $N_{on} > 0$, using Eq. (7), the stationary point ξ is solved by iteration.
(3) Substituting ξ into $q_m(N_{on},R_{on},I)$, q_1 and q_2 is computed.
(4) Substituting ξ, q_1 and q_2 into Eq. (10), the closed-form suboptimal MSLD is available.

5. Fast Closed-Form Suboptimal MLSD Metric

An appropriate initial value ξ_0 is necessary to converge fast when the iteration method is utilized to solve the stationary point ξ using Eq. (7). However, the function $g(\zeta) = \ln\zeta + \sigma^2/2 - \sigma^2(R_{on}\zeta - N_{on}\zeta^2)/\sigma_w^2$ is neither convex nor concave in the interval $\zeta \in (0,+\infty)$, so a local optimum value of ξ may be obtained and besides, the iteration is time-consuming. Consequently, a fast calculation of ξ is a prerequisite for making the suboptimal MLSD metric in Eq. (10) practical.

From Eq. (4), the kth received signal $r[k]$ corresponding to 1 is a Gaussian distribution in the form of $r[k] \sim N(I,\sigma_w^2)$. Assuming that the number of ones in the hypothesis vector s is $N_{on} > 0$, then the distribution of $X = R_{on}$ is $X \sim N(N_{on}I, N_{on}\sigma_w^2)$. Thus, the conditional pdf of R_{on} is given as

$$f_{R_{on}}(x|I,N_{on}) = \frac{1}{\sqrt{2\pi N_{on}\sigma_w^2}}\exp\left\{-\frac{(x-N_{on}I)^2}{2N_{on}\sigma_w^2}\right\},\quad x>0. \tag{11}$$

When I is absence, the conditional mean of R_{on} can be defined as

$$\bar{R}_{on} = \int_0^\infty x\left\{\int_0^\infty f_{R_{on}}(x|I,N_{on})p_I(I)\mathrm{d}I\right\}\mathrm{d}x. \tag{12}$$

As a result, the mean for $R_{on}/2N_{on}$ can be written as $\bar{R}_{on}/2N_{on}$.

From Eq. (11), the conditional pdf of random variable R_{on}^2 is

$$f_{R_{on}^2}(y|I,N_{on}) = \frac{y^{-1/2}}{2\sqrt{2\pi N_{on}\sigma_w^2}}\exp\left\{-\frac{\left(\sqrt{y}-N_{on}I\right)^2}{2N_{on}\sigma_w^2}\right\}. \tag{13}$$

Similarly, the conditional mean for R_{on}^2, in the absence of I, can be defined as

$$\bar{R}_{on}^2 = \int_0^\infty y\left\{\int_0^\infty f_{R_{on}^2}(y|I,N_{on})p_I(I)\mathrm{d}I\right\}\mathrm{d}y. \tag{14}$$

Hence, the mean for $R_{on}^2/2N_{on}\sigma_w^2$ is $\bar{R}_{on}^2/2N_{on}\sigma_w^2$.

In high SNR and weak turbulence conditions taking $N_{on} = 10$, for example, from Eq. (12), the relationship of $\bar{R}_{on}/2N_{on}$ about SNR and S.I. is obtained in Fig. 1. It can be observed that $\bar{R}_{on}/2N_{on} < 1$. From Eq. (14), Fig. 2 shows the relationship of $\bar{R}_{on}^2/2N_{on}\sigma_w^2$ about SNR and S.I. In Fig. 2, the minimum of $\bar{R}_{on}^2/2N_{on}\sigma_w^2$ is 67.7. Hence, from Fig. 2, the conclusion that $\bar{R}_{on}^2/2N_{on}\sigma_w^2 \gg 1$ can be

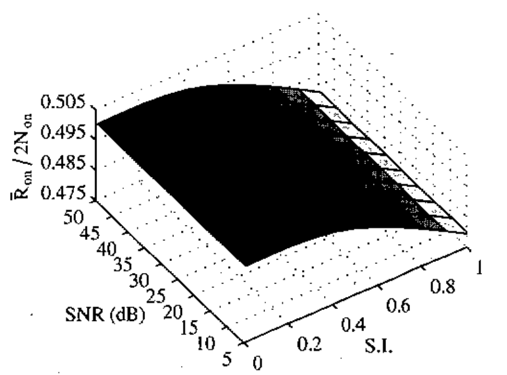

Fig. 1. (Color online) $\bar{R}_{on}/2N_{on}$ as a function of SNR and S.I. when $N_{on} = 10$.

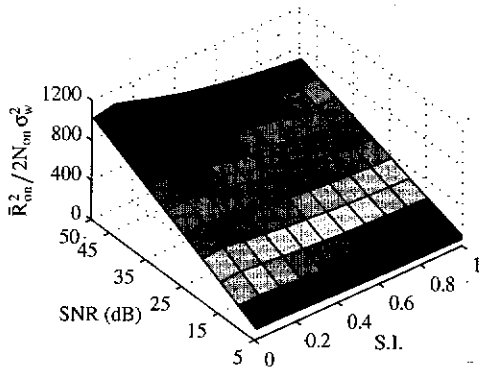

Fig. 2. (Color online) $\bar{R}_{on}^2/2N_{on}\sigma_w^2$ as a function of SNR and S.I. when $N_{on} = 10$.

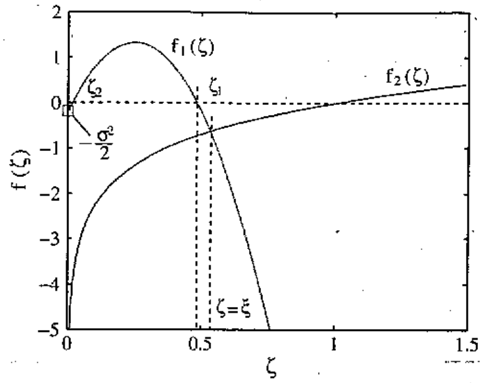

Fig. 4. (Color online) Sketch map about $f_1(\zeta)$ and $f_2(\zeta)$ as functions of ζ.

reached. When N_{on} takes other values, $\bar{R}_{on}/2N_{on} < 1$ and $\bar{R}_{on}^2/2N_{on}\sigma_w^2 \gg 1$ can still be satisfied.

Considering the stationary condition in Eq. (7), let $f_1(\zeta) = -\frac{\sigma^2 N_{on}}{\sigma_w^2}\zeta^2 + \frac{\sigma^2 R_{on}}{\sigma_w^2}\zeta - \frac{\sigma^2}{2}$ and $f_2(\zeta) = \ln\zeta$. For the quadratic equation $f_1(\zeta) = 0$, according to Vieta's Theorem [20], the discriminant is $\Delta = \sigma^4(R_{on}^2 - 2N_{on}\sigma_w^2)/\sigma_w^4$. The symmetry axis of the quadratic function $f_1(\zeta)$ is $\zeta_{sa} = R_{on}/2N_{on}$, so $\bar{\zeta}_{sa} \doteq \bar{R}_{on}/2N_{on} < 1$, and due to $\bar{R}_{on}^2 \gg 2N_{on}\sigma_w^2$, there is $\bar{\Delta} = \sigma^4(\bar{R}_{on}^2 - 2N_{on}\sigma_w^2)/\sigma_w^4 > 0$. Hence, in terms of mean, there are two different real roots for the quadratic equation $f_1(\zeta) = 0$.

On the other hand, if there are real roots for $f_1(\zeta) = 0$, then $R_{on}^2 \geq 2N_{on}\sigma_w^2$. Because the probability $p\{0 < I \leq 0.2\}$ is nearly zero, plus $r[n_i] = I + w[n_i]$, so $r[n_i] > 0.2$. Therefore, there is $R_{on} \triangleq \sum_{n_i \in S_{on}} r[n_i] = \sum_{i=1}^{N_{on}} r[n_i] > \sum_{i=1}^{N_{on}}(0.2)$, i.e., $R_{on} > 0.2N_{on}$, hence $R_{on}^2 > 0.04N_{on}^2$. As a result, if $0.04N_{on}^2 \geq 2N_{on}\sigma_w^2$, then $R_{on}^2 > 2N_{on}\sigma_w^2$ can always be satisfied, thereby there are always two different real roots for $f_1(\zeta) = 0$. Using Eq. (5) yields $\sigma_w^2 = 1/4\gamma = 1/(4 \cdot 10^{SNR/10})$. Combining $0.04N_{on}^2 \geq 2N_{on}\sigma_w^2$, we can obtain $N_{on} \geq 12.5/10^{SNR/10}$. Consequently, $N_{on}^{min} = 12.5/10^{SNR/10}$ is the critical condition for $f_1(\zeta) = 0$, which has two different real roots. The relationship of the minimum window length N_{on}^{min} about SNR is plotted in Fig. 3. It can be observed that there are always two different real roots for $f_1(\zeta) = 0$ if $N_{on} \geq 4$ while $SNR \geq 5$ dB. Moreover, when $SNR \geq 11$ dB, there is just $N_{on} \geq 1$. Hence, when $SNR \geq 11$ dB, quadratic equation $f_1(\zeta) = 0$ always has two different real roots. The two real roots are denoted by $\zeta_1 = (R_{on} + \sqrt{R_{on}^2 - 2N_{on}\sigma_w^2})/2N_{on}$, $\zeta_2 = (R_{on} - \sqrt{R_{on}^2 - 2N_{on}\sigma_w^2})/2N_{on}$, and that $\zeta_1 > 0$, $\zeta_2 > 0$. In the Cartesian coordinate system, $f_1(\zeta)$ and the y axis always intersect at point $(0, -\sigma^2/2)$. For weak scintillation, the scintillation index's interval is S.I. $\in [0, 1]$, thus, $-\sigma^2/2 \in [-0.3466, 0]$. Consequently, there is only one intersection between $f_1(\zeta)$ and $f_2(\zeta)$, namely, the stationary condition in Eq. (7) has only one real root. The sketch map about $f_1(\zeta)$ and $f_2(\zeta)$ is plotted in Fig. 4.

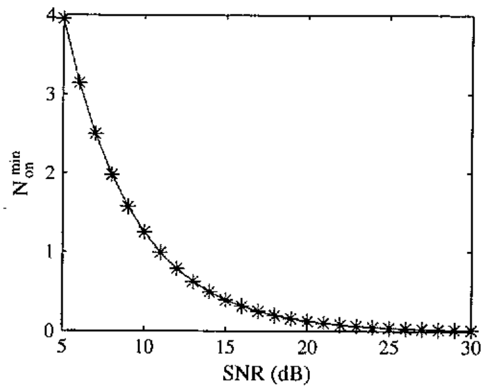

Fig. 3. (Color online) Minimum window length N_{on}^{min} as a function of SNR.

From Fig. 4 it can be observed that the root $\zeta_1 = (R_{on} + \sqrt{R_{on}^2 - 2N_{on}\sigma_w^2})/2N_{on}$ for $f_1(\zeta) = 0$ is close to the x-axis component ξ of the intersection. Hence, ζ_1 can be considered as a good analytic approximation to the stationary point ξ. As well, ζ_1 is also a good initial value if the iteration method is utilized to solve optimum ξ. However, as iteration is time consuming, we treat ζ_1 as the analytic approximation to ξ directly.

As a result, in the high SNR ($\gamma \geq 11$ dB) condition, the algorithm for the fast closed-form suboptimal MSLD metric is summarized as:

(1) For $N_{on} = 0$, there is $M_{subopt}(N_{on}, R_{on}) = 1$.

(2) For $N_{on} > 0$, using $\xi \approx \zeta_1 = (R_{on} + \sqrt{R_{on}^2 - 2N_{on}\sigma_w^2})/2N_{on}$, ξ is obtained directly.

(3) Substituting ξ into $q_m(N_{on}, R_{on}, I)$, q_1 and q_2 are computed.

(4) Substituting ξ, q_1, and q_2 into Eq. (10), the fast closed-form suboptimal MSLD is available.

6. Numerical Results

In this section, the Monte Carlo simulation results for the bit error rate (BER) performance of the suboptimal MLSD receiver in high SNR and weak turbulence conditions are presented. The performance of our closed-form suboptimal MSLD receiver is further compared with that of optimal MSLD receiver and with that of suboptimal MLSD previously reported in [14]. For reference, the detection with genie bound [14], given by

$$\mathrm{BER}_{\mathrm{geniebound}} = E_I\left\{\frac{1}{2}\mathrm{erfc}\left(\frac{I/2}{\sqrt{2\sigma_w^2}}\right)\right\}, \qquad (15)$$

is also included. Furthermore, the performance of the fast closed-form suboptimal MSLD metric is presented. In Figs. 5 through 7, the legend Opt. MLSD means optimal MLSD metric, which is given by Eq. (6). Subopt. MLSDc means closed-form suboptimal MLSD metric given by Eq. (10), in which ξ is obtained by iteration. Subopt. MLSDo is the suboptimal MLSD receiver reported in [14]. Subopt. MLSDfc means fast closed-form suboptimal MLSD metric given by Eq. (10), in which ξ is obtained by analytic approximation.

In Fig. 5, the BER performance of the optimal MLSD receiver and the closed-form suboptimal MLSD receiver for lognormal (S.I. = 0.5) fading channel is shown. Obviously, compared with the close-form suboptimal MLSD receiver of the same sequence length, the optimal MLSD metric outperforms the suboptimal MLSD metric given by Eq. (10). However, the gap between the performances of optimal MLSD metric and closed-form suboptimal MLSD metric is tiny; the SNR loss is less than 1 dB at a given BER. Furthermore, such a gap decreases as the sequence length N increases. For a sufficiently large detection window ($N = 20$), the performance of a closed-form suboptimal MLSD metric is close to the genie bound.

In Fig. 6, the BER performance of the suboptimal MLSD receiver in [14] and the closed-form suboptimal MLSD receiver here for lognormal (S.I. = 0.5) fading is presented. In [14], the performance of Subopt. MLSDo is nearly equivalent to that of the optimal MLSD receiver. From Fig. 6, it can be observed that there is a good agreement between these two suboptimal MSLD receivers, which indicate that the BER of Subopt. MLSDc is nearly equal to that of Subopt. MLSDo.

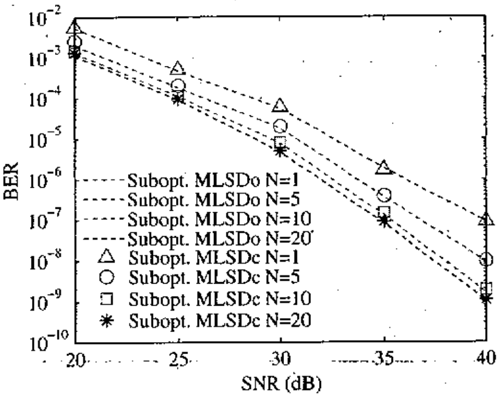

Fig. 6. (Color online) Comparison of the BER performance of the suboptimal MLSD receiver in [14] and the closed-form suboptimal MLSD receiver in this paper for lognormal (S.I. = 0.5) fading channel.

Performance result of Subopt. MLSDfc is given in Fig. 7. The small gaps between the sets of Subopt. MLSDc and Subopt. MLSDfc performance results indicate that the analytic approximation to the stationary point imposes a light degradation in receiver performance. Hence, these results clearly support the analytic approximation to the stationary point. The advantage of Subopt. MLSDfc over other suboptimal MLSD metrics lies in its complete closed-form expression, which comprises simple parameters. Thereby fast computation can be achieved. For comparison, we performed different MLSD metrics for lognormal fading with different scintillation indices, and each metric was executed one million times using Matlab software on a personal computer (PC) platform. The consuming time in seconds for different MLSD metrics is recorded and tabulated in Table. 1. It can be seen that the time consumed by Subopt. MLSDfc is much less than that consumed by Subopt. MLSDo and Opt. MLSD. On average, Subopt. MLSDfc is 54 times faster than Subopt. MLSDo, and 190 times faster than Opt. MLSD. In addition, because more iteration is needed when

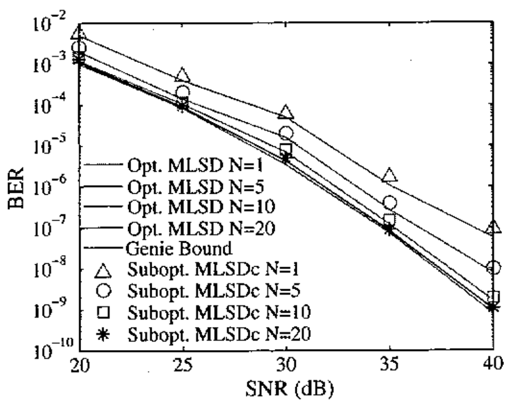

Fig. 5. (Color online) Comparison of the BER performance of the optimal MLSD receiver and the closed-form suboptimal MLSD receiver for lognormal (S.I. = 0.5) fading channel.

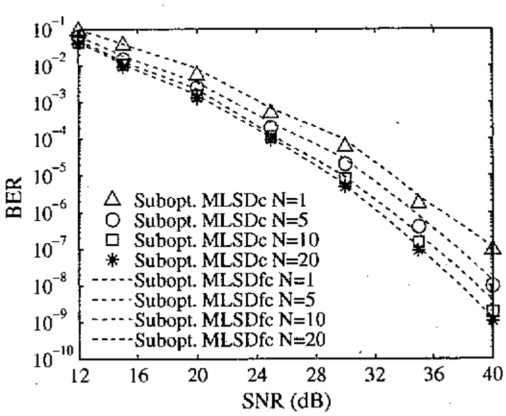

Fig. 7. (Color online) Comparison of the BER performance of the closed-form suboptimal MLSD receiver in this paper and its fast version for lognormal (S.I. = 0.5) fading channel.

Table 1. Computational Time for Different MLSD Algorithms Executed on a PC Platform for Lognormal Fading Channel with Different Scintillation Indices

	S.I. = 0.25	S.I. = 0.5	S.I. = 0.75
$T_{Opt.MLSD}(s)$	66.7673	66.6949	66.9350
$T_{Subopt.MLSDo}(s)$	19.723	18.5767	18.6394
$T_{Subopt.MLSDfc}(s)$	0.3513	0.3514	0.3516
$T_{Opt.MLSD}/T_{Subopt.MLSDfc}$	190.06	189.80	190.37
$T_{Subopt.MLSDo}/T_{Subpt.MLSDfc}$	56.14	52.87	53.01

Table 2. Computational Time of Different MLSD Algorithms Executed on a TMS320DM642 DSP Platform for Lognormal Fading Channel with Different Scintillation Indices

	S.I. = 0.25	S.I. = 0.5	S.I. = 0.75
$T_{Opt.MLSD}$	4.371 ms	4.236 ms	4.403 ms
$T_{Subopt.MLSDo}$	1.061 ms	0.997 ms	1.014 ms
$T_{Subopt.MLSDfc}$	13.996 us	13.931 us	14.025 us

S.I. = 0.25, $T_{Subopt.MLSDo}$ is larger. However, Subopt. MLSDfc has a uniform computational time.

To further demonstrate the advantage of the proposed algorithm, we execute the proposed algorithm and previous optimal and suboptimal MLSD algorithms reported in [14] on a TMS320DM642 DSP platform. The platform has a 720 MHz internal clock. The computational time is recorded and listed in Table 2. From Table 2, it can be observed that Subopt. MLSDfc has the least computational time. On average, Subopt. MLSDfc is 73 times faster than Subopt. MLSDo, and 310 times faster than Opt. MLSD. We attribute this performance improvement to the simple parameters of the closed-form suboptimal MLSD metric. Due to the introduction of the distribution approximation for Subopt. MLSDo, different distribution approximation parameters are necessary to compute how the scintillation index varies. Moreover, Subopt. MLSDo contains some complicated computations, such as computing complementary error function and factorial, which are time-consuming. Therefore it increases the complexity of the suboptimal MLSD metric.

7. Conclusion

In this paper, a suboptimal MLSD in an FSO communications system employing OOK and operating over lognormal fading and a high SNR channel was investigated. A closed-form suboptimal MLSD metric was proposed. This closed-form expression includes parameters that are independent of scintillation index's variation. It consumes uniform time under different scintillation index conditions. When SNR was higher than 11 dB, an analytic approximation to a stationary point was deduced. Using the analytic approximation, a fast closed-form suboptimal MLSD metric was achieved. Simulation results demonstrated that the proposed closed-form suboptimal MLSD metric imposed a light degradation in receiver performance, and the fast closed-form suboptimal MLSD metric brought out less consuming time than other MLSD metrics. Due to good performance, low-complexity, and less consuming time, the conclusion that the proposed closed-form suboptimal MLSD metric and its fast version are excellent alternatives for FSO communications systems operating over lognormal fading channel is reached.

The authors would like to thank the anonymous reviewers whose comments significantly improved the quality of the paper. This work has been carried out with the financial support of the Innovation Project of Chinese Academy of Sciences (Y10532B110).

References

1. M. Uysal, S. M. Navidpour, and J. Li, "Error rate performance of coded free-space optical links over strong turbulence channels," IEEE Commun. Lett. **8**, 635–637 (2004).
2. M. K. Simon and V. A. Vilnrotter, "Alamouti-type space-time coding for free-space optical communication with direct detection," IEEE Trans. Wireless Commun. 4, 35–39 (2005).
3. M. Jazayerifar and J. A. Salehi, "Atmospheric optical CDMA communication systems via optical orthogonal codes," IEEE Trans. Commun. **54**, 1614–1623 (2006).
4. M. Uysal, J. Li, and M. Yu, "Error rate performance analysis of coded free-space optical links over gamma-gamma atmospheric turbulence channels," IEEE Trans. Wireless Commun. **5**, 1229–1233 (2006).
5. M. Cole and K. Kiasaleh, "Signal intensity estimators for free-space optical communications through turbulent atmosphere," IEEE Photon. Technol. Lett. **16**, 2395–2397 (2004).
6. M. Cole and K. Kiasaleh, "Signal intensity estimators for free-space optical communication with array detector," IEEE Trans. Commun. **55**, 2341–2350 (2007).
7. A. Khatoon, W. G. Cowley, and N. Letzepis, "Channel measurement and estimation for free space optical communications," in *Proceedings of IEEE Conference on Communication Theory Workshop* (IEEE, 2011), pp. 112–117.
8. A. Komaee, "Channel estimation for free-space optical communication," in *Proceedings of IEEE Conference on Decision and Control and European Control* (IEEE, 2011), pp. 7299–7304.
9. A. Komaee, "Detection and channel estimation for optical communication over atmospheric turbulent channels," in *Proceedings of IEEE Conference on Information Sciences and Systems* (IEEE, 2011), pp. 1–6.
10. X. Zhu and J. M. Kahn, "Pilot-symbol assisted modulation for correlated turbulent free-space optical channels," Proc. SPIE **4489**, 138–145 (2001).
11. H. Moradi, H. H. Refai, and P. G. LoPresti, "Thresholding-based optimal detection of wireless optical signals," J. Opt. Commun. Netw. **2**, 689–700 (2010).
12. H. Moradi, H. H. Refai, P. G. LoPresti, and M. Atiquzzaman, "A PSAM-based estimator of noise and fading statistics for optimum receivers of free space optics signals," Proc. SPIE **7587**, 1–10 (2010).
13. M. Cole and K. Kiasaleh, "Receiver architectures for the detection of spatially correlated optical field using avalanche photodiode detector arrays," Opt. Eng. **47**, 1–15 (2008).
14. M. L. B. Riediger, R. Schober, and L. Lampe, "Fast multiple-symbol detection for free-space optical communications," IEEE Trans. Commun. **57**, 1119–1128 (2009).
15. M. L. B. Riediger, R. Schober, and L. Lampe, "Multiple-symbol detection for photon-counting MIMO free-space optical communications," IEEE Trans. Wireless Commun. **7**, 5369–5379 (2008).
16. N. D. Chatzidiamantis, G. K. Karagiannidis, and M. Uysal, "Generalized maximum-likelihood sequence detection for

pho ... g free spac ... tical systems," IEEE Trans. Cor ... 3381–3385 (...).
17. X. ... M. Kahn, " ... space optical communication thr ... spheric tur ... ce channels," IEEE Trans. Cor ... 1293–1300 (...).
18. X. ... M. Kahn, " ... v chain model in maximum-like ... ence detecti ... r free-space optical communi-cati ... h atmosphe ... urbulence channels," IEEE Tra ... n. **51**, 509– ... 2003).
19. H. R. Burris, N. M. Namazi, A. E. Reed, W. J. Scharpf, C. I. Moore, M. J. Vilcheck, M. A. Davis, M. F. Stell, M. R. Suite, W. S. Rabinovich, and R. Mahon, "A comparison of adaptive methods for optimal thresholding for free-space optical communication receivers with multiplicative noise," Proc. SPIE **4821**, 139–154 (2002).
20. I. N. Bronshtein, K. A. Semendyayev, G. Musiol, and H. Muehlig, *Handbook of Mathematics*, 5th ed. (Springer, 2005).